

PAPER • OPEN ACCESS

# CFD analysis of turbulent heat transfer and thermal striping phenomena in T-junctions with liquid sodium

To cite this article: P Ferrara and P Di Marco 2017 *J. Phys.: Conf. Ser.* **796** 012009

View the [article online](#) for updates and enhancements.

## Related content

- [CFD analysis of straight and flared vortex tube](#)  
Aman Kumar Dhillon and Syamalendu S Bandyopadhyay
- [A novel approach to CFD analysis of the urban environment](#)  
F Nardecchia, F Gugliermetti and F Bisegna
- [CFD Analysis of the Anti-Surge Effects by Water Hammering](#)  
Tae-oh Kim, Hyo-min Jeong, Han-shik Chung et al.



**IOP | ebooks™**

Bringing together innovative digital publishing with leading authors from the global scientific community.

Start exploring the collection—download the first chapter of every title for free.

# CFD analysis of turbulent heat transfer and thermal striping phenomena in T-junctions with liquid sodium

**P Ferrara<sup>1</sup> and P Di Marco<sup>1</sup>**

<sup>1</sup>Dipartimento Dipartimento di Ingegneria dell'Energia, dei Sistemi, del Territorio e delle Costruzioni, Università di Pisa, Largo L. Lazzarino 1, 56100 Pisa, Italy.

E-mail: [paolo.ferrara@ino.it](mailto:paolo.ferrara@ino.it)

**Abstract.** This paper describes the methodology adopted to perform a CFD analysis with the aim to study thermal striping in T-junctions with liquid sodium; in particular, a portion of the Phenix reactor's secondary circuit has been taken into account, by implementing a detailed 3D model of both fluid and solid domain; RANS and LES turbulence models are used and their results are compared, then frequency analysis of temperature fluctuations has been performed. One of the main results of this analysis is that LES turbulence models are not yet completely reliable in evaluating.

## 1. Introduction

“Thermal mixing” is one of the causes of thermal fatigue failure in nuclear power plants. Thermal mixing characterizes the phenomenon where hot and cold flow streams join, mix and result in temperature fluctuations. Temperature fluctuations cause cyclic thermal stresses and, therefore, they may lead to fatigue cracking of the pipe wall. Thus prediction of thermal field in piping system is an important aspect from the nuclear reactor safety point of view. In order to assess the structural strength, stability and life of such T-junctions, it is essential to know some data with high precision: (i) magnitude of the temperature fluctuations, (ii) characteristic frequencies of temperature fluctuations, (iii) regions of pipe wall where the temperature fluctuations are higher, (iv) attenuation of the temperature fluctuations in the boundary layer near the pipe wall [1]. High thermal fatigue cycles are caused by “thermal striping”, that is a complex thermal hydraulics phenomenon, which generates random fast temperature fluctuations, originating from the incomplete mixing of hot and cold jets of fluid sodium, in the vicinity of adjoining structural wall surface. Thermal striping occurs at a few locations in the hot and cold sodium pools in the reactor assembly, predominantly on the core cover plate of control plug and at mixing ‘Tee’ junctions in the secondary sodium pipelines. The range of frequency of oscillations under thermal striping is found to be 0.1÷10 Hz [2]. A sodium leak detected in a Tee junction of the fast breeder reactor Phenix was the starting point of an IAEA international benchmark on thermal fatigue [3]. Hot sodium flow is injected by a small pipe in a large cold pipe, the temperature fluctuations due to the mixing downstream of the Tee have initiated a crack. Nowadays CPU resources are much higher than 10-15 years ago and new turbulence models have been developed, so it is interesting to assess them in the given problem.

Therefore a portion of the Phenix reactor's secondary circuit has been taken into account, by implementing a detailed 3D model (figure 1) [3]. The purpose of this study is: (i): to build a computational grid that allows to reach a good compromise between reduced computational time and high quality results; (ii): to evaluate turbulent heat transfer from liquid sodium to solid wall; (iii): to

study the time-averaged behaviour of the fluxes in the mixing region for this specific case, evaluating thermal striping phenomena; (iv): to perform very accurate calculations, in order to compare numerical results with experimental data coming from the real nuclear facility, these data are listed in IAEA TECDOC 1318, [3]. Simulation results must be compared with experimental data, that are detected in real Tee by using 15 thermo-couples (called TCs for the sake of simplicity); but, in present work, only 5 of them are considered, because they are the only ones that detect some temperature fluctuations with respect to an unperturbed condition (i.e.:  $T_{ref} = 340^{\circ}\text{C}$ ).

Our simulations will be performed by using both RANS and LES turbulence models: the goal of RANS calculations is mainly to find: (i) the best grid and (ii) the best turbulence model to perform the final step of the analysis, so, at this point, we just want to make a *relative* comparison between results and it is crucial to do it as fast as possible. In other words: at this point it not important if the results of the such calculations are or not close to experimental data. On the contrary, when we perform the final step of the analysis, (i.e. a LES calculation with the best grid and the most suitable LES model), the goal is to obtain temperature data comparable with those contained in IAEA TECDOC 1318.

## 2. Fluid model geometry

The first step of a CFD calculation is the creation of a geometry, that allows to handle accurately the case to study; in particular, the T-junction of [3] can be modelled as in figure 1. The reference system is oriented as described in [3]: X axis is vertical and coincident with main pipe axis in the mixing region, Z axis is horizontal. Different colours of surfaces in figure 1 underline that those surfaces can be handled separately during the definition of the CFD problem, so that different boundary conditions can be assigned in different zones of the fluid domain. In figure 1, X axis is vertical and Z axis is horizontal: they lie on the symmetry plane.

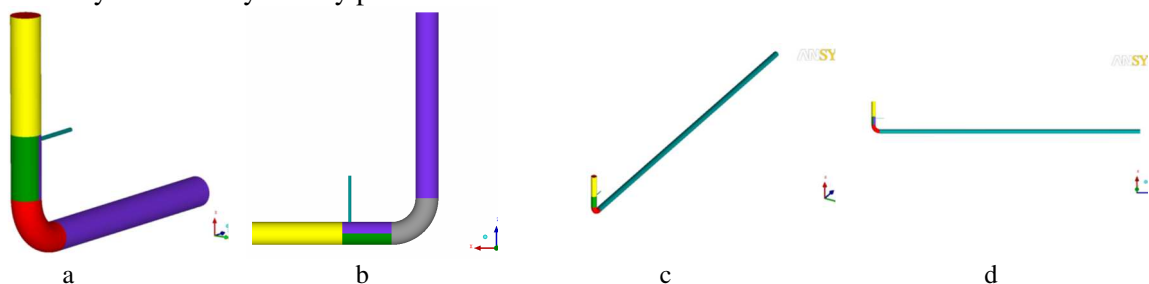


**Figure 1.** Geometry for CFD calculation: a: isometric view; b: lateral view. Geometrical model with long horizontal pipe: c: isometric view; d: lateral view.

When performing RANS simulations, geometrical model of figure 1.a and 1.b suits our purposes, whereas, when performing very accurate LES calculations, [4], more realistic initial and boundary conditions are needed, in particular at the inlet, because, inside the mixing region, turbulent flux should be completely developed. If we use ANSYS CFX 12, it is not possible to simply add a random velocity distribution to the mean fluid velocity at the inlet (i.e.: to the laminar inlet conditions). Therefore, for the last calculation, the upstream region of the main pipe has been modified, by increasing the horizontal tube length to let the turbulent flow be fully developed. To estimate such length increment, we proceed in this way: it is known that the entrance length (here called  $L_{entrance}$ ) needed to reach a fully developed turbulent flow (from an uniform flow at the pipe inlet) can be evaluated as follows [5]:  $L_{entrance} \approx 4.4 \cdot D \cdot (\text{Re})^{1/6}$ , where  $D$  is the hydraulic diameter of the pipe; thus, if  $\text{Re} \approx 6.8 \cdot 10^6$ , as in our case, then:  $L_{entrance} \approx 55D$ , therefore the horizontal pipe should be at least 28m long, instead of 4m. Hence, to be more conservative, we decided to use a 32m long horizontal pipe (i.e. 8 times the original length), in order to let the turbulent flow fully develop, starting from laminar conditions at the “new” inlet, that is now far downstream. “Laminar conditions”, in this case, means: uniform velocity profile and constant temperature along the inlet surface.

### 3. Computational grids of fluid and solid domain for RANS and LES calculations

The fluid domain of mixing Tee is meshed with Hexa-type elements, in order to better control the mesh quality. ANSYS ICEM-CFD allows to create Hexa meshes, using “blocks”, namely splitting the entire domain into simpler parts, each of them can be seen as a *big*-Hexa-type element, so that this can be easily split into many *smaller* Hexa-type elements. In Phenix Tee case, the fluid volume is divided into three parts, as one can see in figure 2. The first goal of the present work is to create a global mesh, that may lead to a compromise between good quality calculation results and low computational cost, thus saving CPU time. To reach this goal many attempts were done, in particular to assess the parameter  $y^+$  in the mixing region, by varying the parameters “ $n$ ” (number of nodes along an edge) and “ $r$ ” (ratio between consecutive nodes), for near-wall blocks.

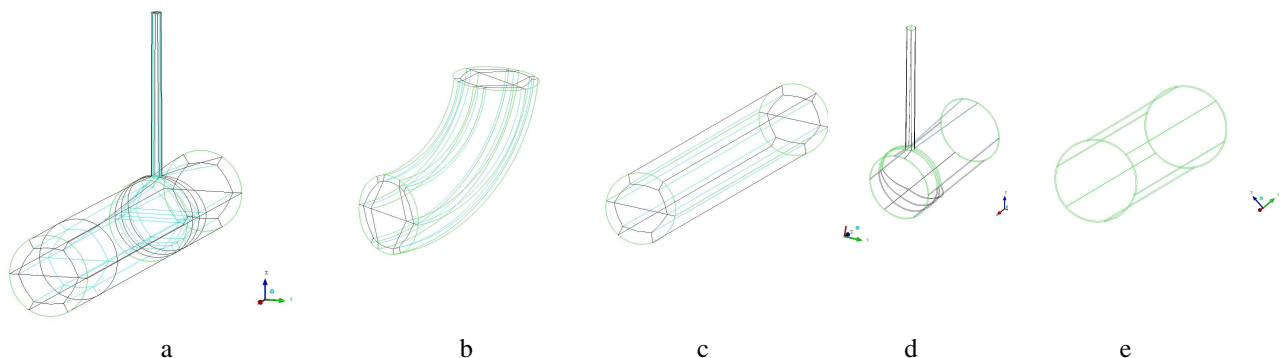


**Figure 2.** Mesh blocks: a: mixing region: vertical pipe and branch pipe. Upstream region: b: elbow; c: horizontal pipe. Solid wall blocks: d: injection; e: downstream zone.

In other words, mesh refinement in circumferential and axial directions of main pipe can be coarser than refinement in radial direction, but, at the same time, it is needed to satisfy requirements for computational grids to be used in LES calculations. In particular,  $y^+$  should be close to 1 in near-wall region, at least in the zone of interest, i.e. the mixing region, near the OXZ plane, after the injection. In order to improve simulation results, it is necessary to reach a good *mesh quality* [6] in the mixing region. Conduction inside pipe solid wall is calculated, but only in the region downstream hot and cold fluids intersection, i.e. only where such analysis is really needed, so that a more accurate analysis of the T-junction problem can be performed, thanks to the Conjugate Heat Transfer (CHT) tool [7]. Main features of these grids,  $y^+$  distribution and results of preliminary RANS calculations are summarized in [8,9]: looking at figure 7 of [8], that is referred to the finest grid for RANS and LES calculations, we can see that average value of  $y^+$  is essentially around unity, in proximity of the junction. Besides, main features of final grids (called A1, A2 and A3) can be found also in this paper, in table 2. In RANS and LES run, thermal conduction inside pipe solid wall has been calculated (in the mixing region) using a 3D domain of the AISI 304 stainless steel wall. In order to guarantee a good mesh quality, the solid volume is divided into two sub-volumes: injection zone and downstream zone, as one can see in figure 2.d and figure 2.e; see also [8,9].

## 4. RANS Calculations

### 4.1 RANS Calculations planning

RANS calculations are divided in 3 groups: (i) the first one is aimed to compare the results of the calculations performed with 16 grids (described in [8]), in order to build the final grids for LES calculations (called A1, A2 and A3); (ii) the second one is performed by using the best grid of the previous group, in order to compare different turbulent models: Reynolds Stress Model (RSM), Shear Stress Transport (SST) and  $k-\epsilon$  method with standard coefficients, (one low-resource consuming RANS calculation is performed for each of the final grids); (iii) the third one is constituted by a single calculation performed with the final grid to be used for LES runs, in order to describe the mean flow: this is useful also to find a good initial condition for LES calculations.

It is well known that an unsteady RSM approach should be useful to verify the natural steadiness of the phenomenon, but we also know that this capability is better verified by LES models, so we decided to limit the use of RANS simulations to steady-state cases, in order to evaluate only the average temperature profile. The computational domain of the first group is constituted only by the fluid mesh, in order to save CPU time, whereas the computational domain of the other 2 groups are constituted by both solid and fluid mesh, in order to provide better results. Only the last RANS calculation (group (iii)) has been performed by using the 32m upstream horizontal tube, see figure 1.c and 1.d.

#### 4.2 Main features of RANS calculations

In first RANS calculations, non-dimensional wall distance ( $y^+$ ) is evaluated for a steady-state case of a simplified model, where solid wall of the pipe is not included in the model, but the action it produces near wall in sodium temperature profile is taken into account, by assessing the wall heat transfer coefficient on the cylindrical surfaces of the fluid domain. Main features of the RANS calculations may be summarized as follows: (i) RANS turbulence models: steady-state RSM, SST and  $k-\varepsilon$  method with standard coefficients (see sec. 4.1); (ii) main inlet has a mass flow of 800kg/s and a temperature of 340°C; (iii) branch-pipe inlet has a mass flow of 7kg/s and a temperature of 430°C; (iv) outlet has a mass flow of 807kg/s; (v) cylindrical surface of fluid domain is considered as a solid wall, with heat transfer coefficient ( $h$ ) of 16 W/m<sup>2</sup> K and outside temperature of 25°C.

Material properties for liquid metal and solid are considered constant and they are extrapolated from data of International Nuclear Society Council (INSC) at an intermediate value between hot and cold sodium temperature: for first calculations it is chosen to use the mean value between 340°C and 430°C, that is 385°C. Convergence criteria for each steady-state calculation is that the normalized Root Mean Square (RMS) values of residuals must be under  $10^{-4}$ . Turbulent heat flux is modelled by using the so called “thermal energy” model implemented in ANSYS CFX 12.1, see [10]. Concerning numerical schemes features, ANSYS-CFX adopts an “unstaggered” grid scheme, RANS equations are discretized by using a first order backward Euler scheme and the convective term is modelled by using a first order “upwind” scheme. Sometimes first order schemes are not very accurate, but, in our case, results of RSM simulations are very close to experimental data (see figure 3.a), thus this approximation suits our purposes, allowing also to save CPU time. For further details, see [10].

### 5. LES Calculations

#### 5.1 LES Calculations planning

First of all, a sensitivity analysis has been performed by comparing different computational grids and different subgrid models, only to make only a *relative* comparison between grids and numerical models, even if the calculated values could result still far from experimental data. On the contrary, the final step of LES calculation campaign consists of an extension of simulation time of the best case (that is: the best computational grid with the best subgrid model), in order to collect enough data for *statistics*, to make a good comparison between calculated and experimental data. Main features of computational grids for sensitivity analysis can be found in table 2 and in [9].

At the end of these simulations, the best subgrid model between Dynamic, WALE and Smagorinsky model can be chosen, so that its simulation time can be *extended* up to 60s: to be more precise, the final LES calculation must be *repeated* from the beginning, because the initial condition for the final run should be as accurate as possible. The long duration of simulation time is absolutely needed, because: (i) it allows the thermal wave to completely cross the solid wall of the pipe in radial direction, that is: about 12s, (because the TCs are placed outside such wall), therefore the total time extension of the simulation must be much greater than 12s; (ii) it is necessary to collect enough data for *statistics* to make a good comparison between calculated and experimental data; besides, it is necessary to *cut* the initial transient from the analysis, i.e. at least the first 12s, if looking at figure 9. So, in our case, the transient due to the approximate initial conditions seems to be much greater than *one* residence time (i.e. the amount of time to cut, as recommended in literature [11]).

Therefore, it is useful to define a simple criterion in order to distinguish between such *initial transient* and the *stable solution*. It was chosen to apply this criterion to *each* TC: (i) the time-averaged temperature value has been evaluated, starting from 57 different initial instants of time, thus obtaining 57 values (named: “value 1”, “value 2”, ... , “value 57”), calculated as follows: “value 1” is the time-averaged temperature between “simulation time = 1s” and “simulation time = 60s” (i.e. the last one), for a given TC; “value 2” is the time-averaged temperature between “simulation time = 2s” and “simulation time = 60s”, for a given TC; and so on. (ii) Such mean values must be normalized by dividing them for an appropriate mean temperature value, related to a given TC (because this value is different for each TC). This is called *asymptotic* value and it can be approximated with the mean temperature value between the 57 values previously described (“value 1”, “value 2”, ... , “value 57”). (iii) The time interval of the *stable* solution could be defined as the time interval where fluctuations of normalized mean temperature are less than 0.5% with respect to the *asymptotic* value; (iv) To be conservative, the longest initial transient between those relative to the 5 TCs should be chosen.

At this point temperature fluctuations profile should be correctly evaluated, thermal striping phenomena occurring in T-junctions with liquid sodium can be accurately studied and also frequency analysis can be correctly developed.

## 5.2 Main features of LES calculations

Main features of LES calculations in present work may be summarized as follows: (i) LES subgrid model is implemented in ANSYS CFX, [10]: classic Smagorinsky, Dynamic or WALE: they are all used for sensitivity analysis; then, the best one is chosen for the final run; (ii) total simulation time: 5s (for sensitivity analysis) or 60s (for the final simulation), as it was explained in the previous section; (iii) boundary conditions are the same used in RANS calculations. Time-step size should be less than 0.00005s, to maintain Courant Friedrichs Lewy (CFL) number below 1, in order to capture small scale phenomena, but, if this value would be adopted for the entire transient, computational cost would be huge, so this value has been used only at the beginning of each transient, that is: between 0s and 0.1s, whereas time-step has been increased to 0.0001s between 0.1s and 0.3s, then it has been increased to 0.0002s until 12s and, finally, time-step has been increased up to 0.001s until the end of the simulation. Doing so, CPU time for the final calculation has been over 1 month. Initial condition for *each* LES calculation (*but the last one*) is the result of a steady-state RANS  $k-\epsilon$  calculation performed with the *same grid* of the corresponding LES calculation, in order to avoid interpolation errors at the beginning of the LES transient; whereas, initial condition for the *last* LES calculation is given by the result of a calculation performed using the RANS turbulence model that better simulates the mean flux of the mixing Tee. Here the convective term is modelled by using a central difference scheme. The unsteady term in LES calculations is modelled by using a second order backward Euler scheme. Convergence criteria for each time-step is that the normalized RMS values of residuals must be under  $10^{-4}$ . *Experimental* data of temperature are taken every 0.001s, therefore, *computed* temperature data must be extrapolated with the same frequency (i.e. 0.001s), in order to make a correct comparison.

In sec. 1, it has been already remarked that the comparison between simulation results and experimental data should be done in correspondence of 15 TCs, even if, in present work, only 5 of them are considered, because they are the only ones that detect some temperature fluctuations with respect to an unperturbed condition (i.e.:  $T_{\text{ref}} = 340^{\circ}\text{C}$ ) [3]; their position is reported in table 4 of [8]. Besides, an “*interface point*” (called “Interf TC”) is defined in correspondence to each TC, namely a point that lies on the interface between fluid and solid, in such a way that it has the same X and Y coordinates of the corresponding TC, but  $Z = 0.247\text{m}$  at the interface, whereas:  $Z = 0.254\text{m}$ , for each TC, in fact TCs lie on the external surface of the pipe wall.

## 6. Results and discussion

In our case, the best RANS model to simulate the *mean flux* inside T-junction is a steady-state RSM, because it provides mean temperature values that are very close to the experimental data (figure 3.a), in fact the difference between experimental and calculated data is less than  $1^{\circ}\text{C}$  over about  $400^{\circ}\text{C}$ , for



each TC but the first one. So RANS RSM turbulence model seems to be the best initial condition (IC) to start the final LES calculation, even if it has a very high computational cost, when compared to other RANS models. In RANS and LES calculations, material properties can be considered constant with temperature, in particular this approximation is valid for sodium density, because Richardson number is less than  $10^{-3}$  inside the mixing region: it means that buoyancy effects are negligible, according to the criterion suggested by Jackson for liquid metals in ascending pipes [12]; so, in this case, forced convection is dominant. In fact, if we consider a steady-state  $k-\varepsilon$  case, where density is variable with temperature, we can notice that density variations are negligible, because their maximum variation (normalized with medium density) is less than 2.5% (see figure 4.a). Now main results of a steady-state calculation performed with RSM turbulence model are briefly summarized and, when necessary, they are compared with the corresponding results obtained with LES subgrid turbulence models.

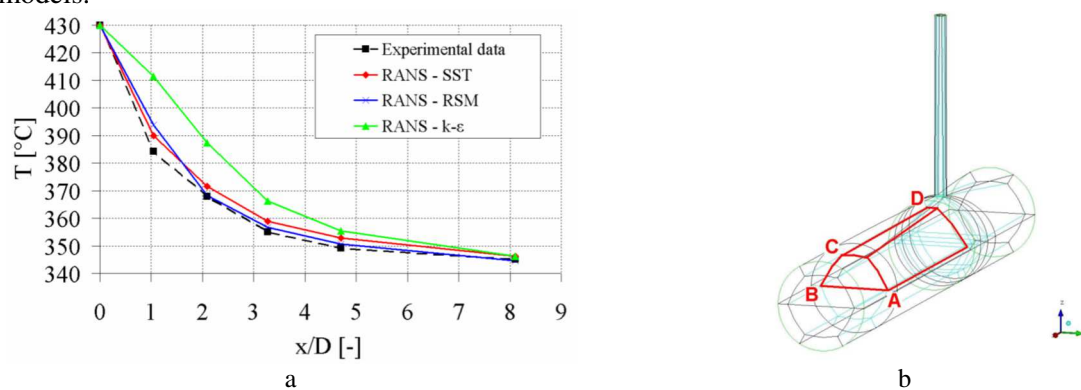


**Figure 3.** a: Comparison between 3 RANS turbulence models: RSM, SST and  $k-\varepsilon$ ; b: Main inner block in mixing region, useful to summarize most important features of final grids, listed in Table 2.

**Table 1.** Classification of mixing flow types as a function of  $M_R$ .

Jet type	$M_R$ value
Wall jet	$90 < M_R$
Re-attached jet	$20 < M_R < 90$
Turn jet	$2.5 < M_R < 20$
Impinging jet	$M_R < 2.5$

**Table 2.** Main features of the 3 final grids in the mixing region; (\*):  $n$  and  $r$  are relative to the near-wall block above the segment CD.

Case name		A1	A2	A3
N° of elements (x $10^6$ )		2.25	3.14	2.60
$n$ (*)		28	30	29
$r$ (*)		1.25	1.25	1.25
N° of elements in main inner block, see figure 3.b	AB	24	24	24
	BC	24	40	34
	CD	147	168	147

Comparing figure 4.b and figure 4.c, it is possible to notice a non-negligible temperature difference between the solid-liquid interface and the outside wall (about  $10^{\circ}\text{C}$  for corresponding axial and azimuthal positions), because this thin wall made of stainless steel (only 0.007 m thick) acts as a damper for internal temperature variations, being them either in time or in space. Such variations are damped by a quasi-exponential law through the wall thickness: it means that TCs, placed outside wall thickness, are capable of detecting only strongly attenuated temperature fluctuations with time. In fact, for the final LES simulation, the time evolution of temperature in 5 TCs is shown in figure 9.a, whereas the same variables in 5 corresponding “interface points” are plotted in figure 10, showing how big the damping can be. In fact, the peak-to-peak temperature difference can be greater than  $100^{\circ}\text{C}$  at the solid-fluid interface, whereas it rarely becomes greater than  $5^{\circ}\text{C}$  outside solid wall.

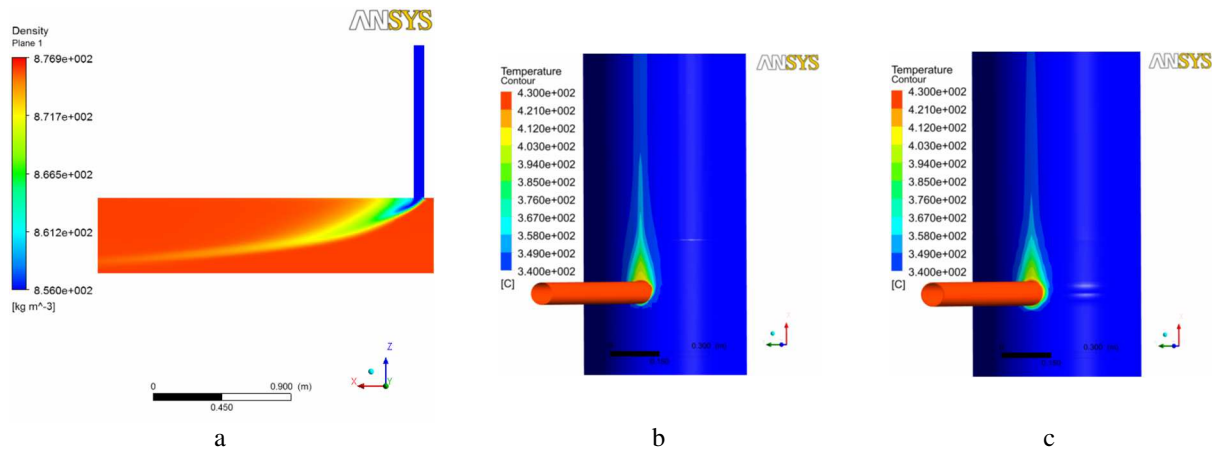


**Figure 4.**a: Sodium density in OXZ plane; b: Temperature on the interface between solid and fluid domain; c: Temperature outside solid wall.

According to [13], the pipe section in the mixing region can be divided in 4 parts (see figure 5.a): region “A”, called “*pure tap water*”, where RMS temperature values are low; region “B”, called “*mixing zone*”, where there is a mixture with high RMS temperature values; region “C”, called “*pure DI*”, adjacent to region “B”, where RMS temperature values are low, (similar to region “A”); region “D”, called “*separation region*”, placed in the region close to the branch pipe: it contains 2 counter-rotating vortices which rule the recirculation region. Such vortices can be clearly observed in Phenix Tee case, see figure 5.b.

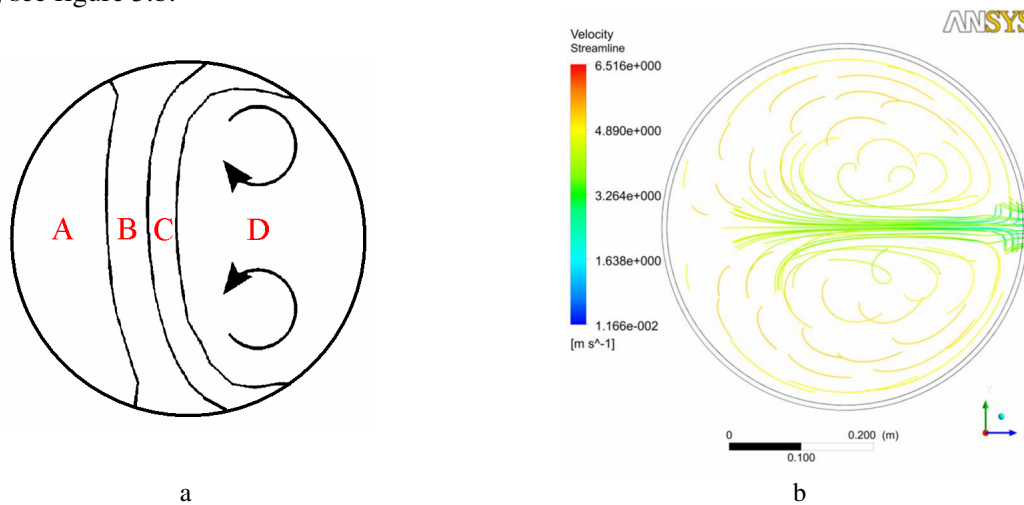


**Figure 5.**a: the mixing region can be divided into 4 parts; b: streamlines projected on OYZ plane; they start from a geometrical OYZ plane located at X = 0.9 m.

According to [14], if we consider a T-junction with 90° bend, mixing flow depends on the value of a non-dimensional parameter, called “momentum ratio”, defined as:

$$M_R = \frac{\rho_m U_m^2 \cdot (D_m \cdot D_b)}{\rho_b U_b^2 \pi \cdot (D_b / 2)^2}, \quad (1)$$

where  $\rho_m$  and  $\rho_b$  are, respectively, “main” and “branch” flow densities,  $U_m$  and  $U_b$  are the mean flow velocities of “main” and “branch” fluxes, whereas  $D_m$  and  $D_b$  are the hydraulic diameters of “main” and “branch” fluxes. Different values of  $M_R$  define different types of mixing flow, as it is



shown in table 1; one can have either a “*wall jet*”, if the branch flux remains attached to the wall of the main pipe, or a “*re-attached jet*”, if the branch flux first separates from the wall of the main pipe and, then, it re-attaches to it, or a “*turn jet*”, if the branch flux separates from the wall of the main pipe and it remains close to the axis of the main pipe, or an “*impinging jet*”, if the branch flux hits the wall on the opposite site of the injection zone. Using equation (1), where:  $\rho_m \approx 876.9 \text{ kg/m}^3$ ,  $\rho_b \approx 856 \text{ kg/m}^3$ ,  $U_m \approx 4.6 \text{ m/s}$ ,  $U_b \approx 2.1 \text{ m/s}$ ,  $D_m = 0.494 \text{ m}$  and  $D_b = 0.068 \text{ m}$ , it is found that  $roc \approx 43$ , so, according to table 1, flux type is in the range of “*re-attached jets*”. Anyway, we have to remark that the threshold values used in table 1 are referred to the case of a T-junction without any elbow, according to [14], whereas the T-junction considered in IAEA benchmark shows an elbow just downstream the secondary flux injection; therefore such threshold values can only be considered as a first reference to distinguish between different types of mixing regions, in fact they could be shifted up or down, by the presence of an elbow. So it is difficult to predict exactly the type of mixing flow, even if it should be closer to a *turn jet*, because the presence of an elbow bends the streamlines through the extrados of the curved pipe, therefore such streamlines are deviated to the opposite side of the injection zone, so they are likely to push also secondary flow away from the wall that is close to the branch pipe. Besides, the calculated flow can have different features depending on different turbulence models adopted, because of their different capacity to evaluate mixing, in fact, mean flux calculated by using RANS turbulence models behaves as a *turn jet* (figure 6.a, figure 7.a, figure 7.c, figure 8.a), [14], because the hot plume arranges near the main pipe axis, downstream the secondary injection. Therefore the mixing region gets away from the main pipe wall and its shape is very massive and almost cylindrical: this is due to the low capacity of RANS turbulence models to evaluate mixing phenomena between hot and cold fluids (figure 7.a, figure 7.c). We remind that “mixing zone” can be defined as an iso-surface with a temperature equal to  $T_{\min}$  plus 5% of maximum  $\Delta T$  between hot and fluid, therefore, in this case: iso-surface with  $T \approx 345^\circ\text{C}$ . This can be useful to better understand figure 7.a and figure 7.b. On the contrary, instantaneous flow calculated by using LES subgrid models behaves as a *wall jet* (figure 6.b, figure 7.b, figure 7.d, figure 8.b, [14], because of the greater capacity of such models to evaluate mixing phenomena between hot and cold fluids, in fact the mixing region is located very close to the solid wall and its shape is very diffused and constituted by many small structures (figure 7.b, figure 7.d). So, it seems that neither RANS nor LES simulations can reproduce correctly the shape of the mixing region, because, as it was anticipated above, the real behaviour of the mixing region should be a way in the middle between the results found with different turbulent models, that is: it should be closer to a “*re-attached jet*”.

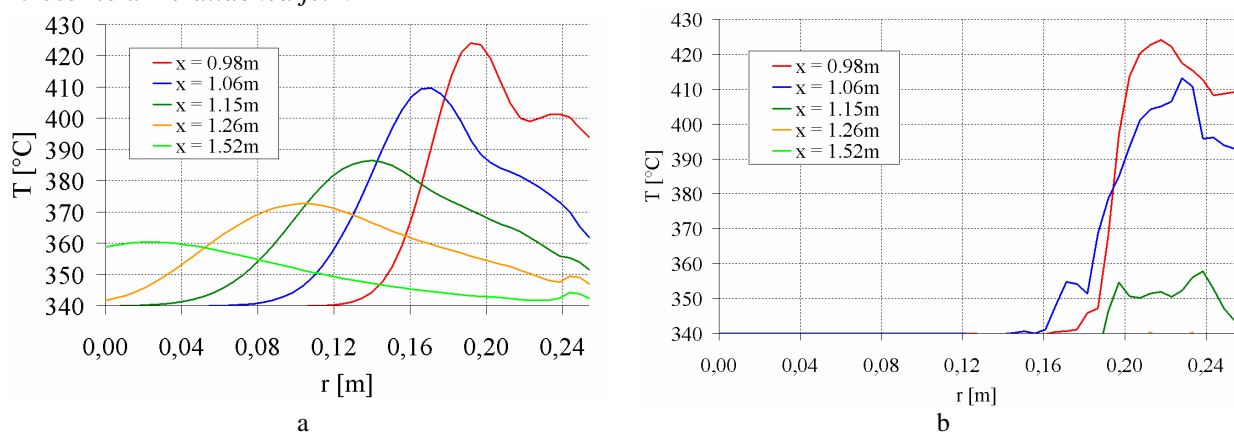


**Figure 6.** Temperature profile versus pipe radius for 5 TCs: a: RANS RSM turbulence model. Here mixing zone penetrates into the central part of the main pipe (see green curve); b: LES Dynamic subgrid model, medium values: here mixing zone is only in near-wall region.

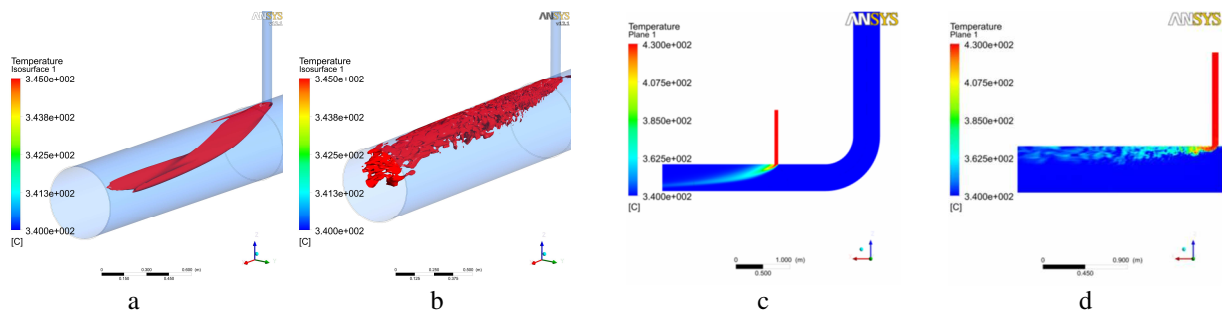


**Figure 7.** Mixing zone: a: RANS RSM turbulence model; b: LES Dynamic subgrid model, after 12s. Temperature in OXZ plane: c: RANS RSM turbulence model; d: LES Dynamic model, after 12s.

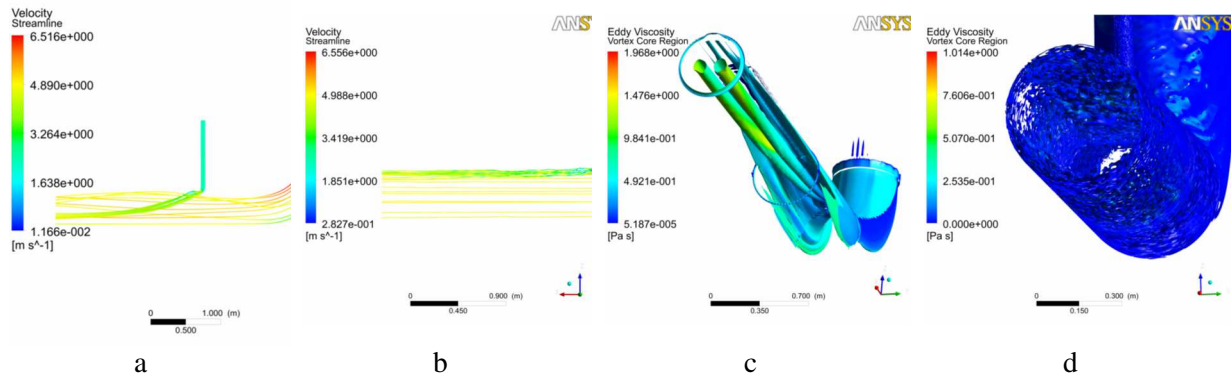


**Figure 8.** Streamlines in OXZ plane: a: RANS RSM turbulence model; b: LES Dynamic model, after 12s. c: Vortices shape, RANS RSM turbulence model; Q-criterion [10]:  $Q = 22 \text{ s}^{-2}$ , time-averaged values; d: Vortices shape, LES Dynamic subgrid model; Q-criterion:  $Q = 68 \text{ s}^{-2}$ , instantaneous values after 12s.

In figure 6.a, referred to a RANS simulation, we can see that the bright green line, referred to TC 6 (i.e.: the TC placed farther from the secondary injection) shows a temperature increment of about  $20^\circ\text{C}$  close to the main pipe axis (that is: where the radius “r” is close to 0 m); it means that, in such region, a hotter plume of liquid sodium is flowing through the colder bulk of fluid, and it is another prove that the RANS models underestimate mixing phenomena. This does not happen in LES simulation, as it can be shown in figure 6.b, where the bright green line, referred to TC 6, lies in the

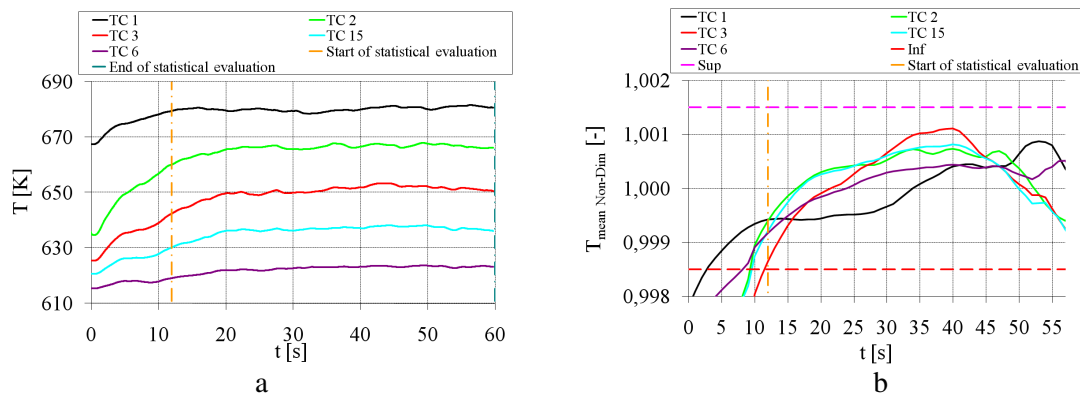


**Figure 9.** a: Time evolution of temperature in 5 TCs: initial transient is at least 12s long; b: Visual representation of a simple criterion to distinguish between the initial transient and the stable solution: for further details, see sec. 5.1.

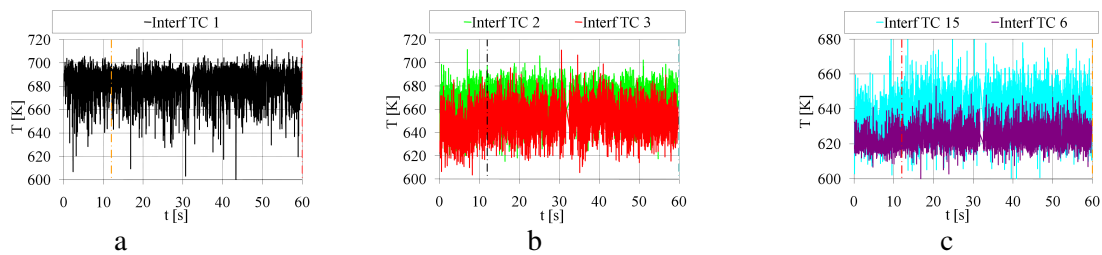


**Figure 10.** Time evolution of temperature in 5 interface points: a: Interf TC 1; b: Interf TC 2 and Interf TC 3; c: Interf TC 15 and Interf TC 6. Statistical evaluation: from  $t = 12$ s to the end.

horizontal axis, when the flow is close to the main pipe axis, therefore the mean temperature is very close to  $340^{\circ}\text{C}$ , so it means that mixing phenomena are confined in the near-wall region, as effectively happens in the real case. Also the vortices shape is very different between RANS and LES turbulence models, in fact, in the first case, time-averaged values are taken into account, so we can find 2 big counter-rotating vortices over the mixing region (figure 8.c), while, in the second case, instantaneous values are taken into account, so we can find many small eddy structures, that are very close to the solid wall (figure 8.d). The time-step extension is very important in the evaluation of the temperature fluctuations, because, if it does not satisfy the Courant-Friedrich-Levy condition, turbulence is damped, therefore temperature peaks can be attenuated, so time-step should be very small. On the other side, it is necessary to simulate a long transient in order to collect enough data for a correct evaluation of statistics, therefore, a good compromise must be found, if we want to fulfil 2 opposite requirements. Using the criterion described in sec. 5.1, the initial transient extension is about 12s (see figure 9.b), that is, the stable solution seems to start after about six residence times, in fact, after that time, mean normalized temperature values in correspondence to each TC are very close to 1; it means that the first 12s of this LES simulated transient shall not be taken into account to evaluate statistics. Besides, it is needed to wait that the thermal wave completely crosses the solid wall of the pipe, if we want to correctly evaluate the statistic values, because TCs are placed outside such wall.

Results of calculations performed with LES turbulence models *for sensitivity analysis* show some difference with experimental data, in fact RMS temperature fluctuations are under-estimated by some degrees, whatever is the grid and/or the LES subgrid model adopted. RMS temperature fluctuations are more sensitive to the extension of horizontal pipe, i.e.: 4m vs. 32m length (figure 12.a), than to grid refinement (figure 11.a) or to LES subgrid model (figure 11.b); in fact enough space shall be included in the upstream region of the mixing Tee to let the turbulent flow to be completely developed. In this problem, the finest grid (A3, see table 2) shows the best *qualitative* profile of RMS temperature fluctuations (figure 11.a), so it is chosen to perform the subsequent runs; besides, the

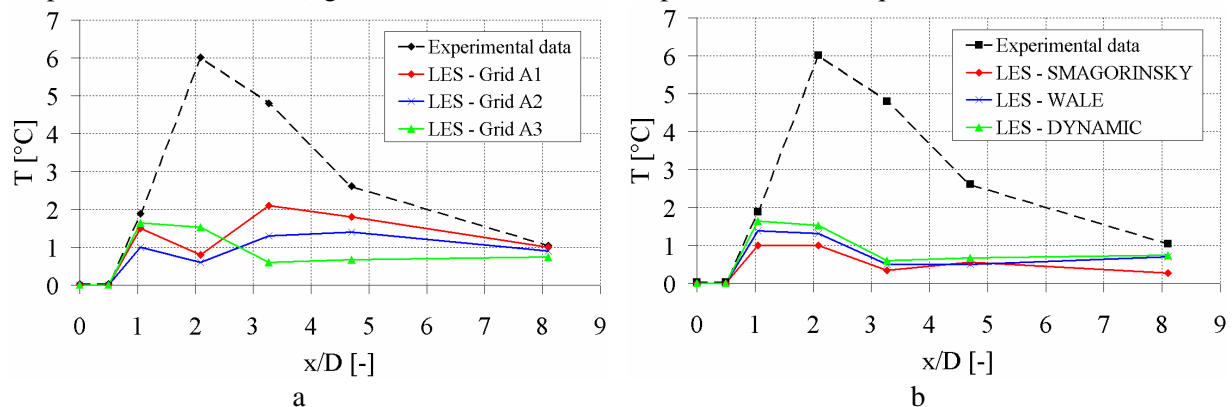


**Figure 11.** RMS values of temperature fluctuations: comparison between experimental data and calculated data: a: different grids; b: different LES subgrid turbulence models.

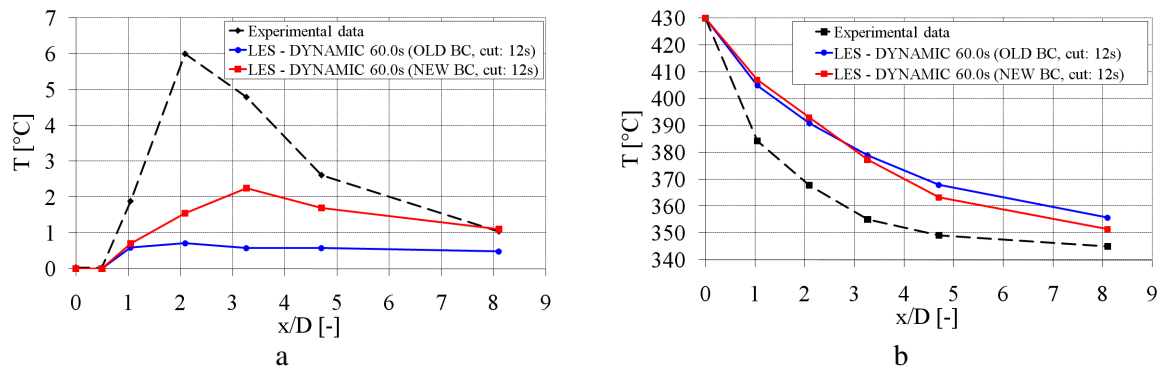


**Figure 12.** Different BCs: “OLD BC” means: simulation with 4m long horizontal pipe; “NEW BC” means: simulation with 32m long horizontal pipe. Comparison between experimental data and calculated data: a: RMS values of temperature fluctuations; b: mean temperature values.

Dynamic subgrid model appears to be the best one to correctly evaluate RMS temperature fluctuations, even if the results produced by the 3 subgrid models are very similar (figure 11.b). Looking at figure 12.a, it is useful to remember that RMS values of temperature fluctuations could be much higher, if we would consider also the initial transient, because, in that case, the solution would be *quickly* changing to evolve from ICs to quasi-stationary values, whereas we are only interested in to the stable solution. Unfortunately, the code provides data that are quite lower than experimental measurements; it means that RMS values of temperature fluctuations are *under-estimated* by the code, if compared with experimental data (see red line in figure 12.a); on the contrary, mean temperature values are *over-estimated* by the LES model of about 15°C, see figure 12.b. Anyway, we can observe that the adoption of a more correct boundary condition at the inlet, (called “NEW BC”, i.e. simulation with a “32m horizontal pipe”), is useful to improve results of both RMS and mean values of temperature, with respect to the case with “4m horizontal pipe”, (called “OLD BC”), i.e. the case with the non-correct inlet condition, (see, the blue line in figure 12.a and figure 12.b). Nevertheless, the differences with experimental data still remain appreciable, probably because of the following reasons: *first*: the extension of time-step is high in order to save CPU time, but it probably damps too much turbulent oscillations, *second*: it is possible that the LES subgrid model adopted is not capable of correctly modelling thermal striping phenomena, in particular: the fluctuations of turbulence structures; *third*: the grid resolution is very fine in radial direction, but it is still quite rough in axial and azimuthal direction, (again, this choice has been taken to save CPU time).

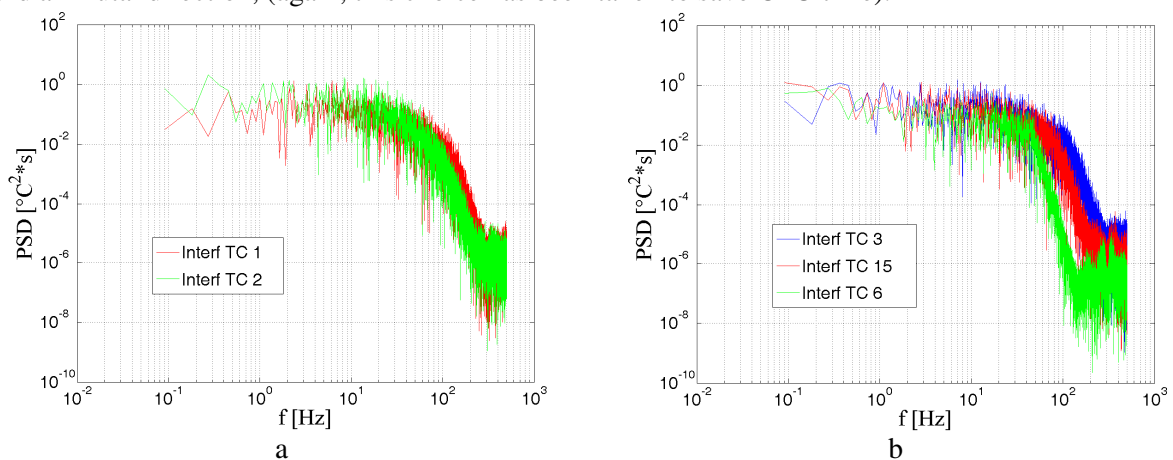


**Figure 13.** Frequency analysis: Power Spectral Density (PSD) vs. frequency in various positions at the interface between solid and fluid domains: a: Interf TC 1 and Interf TC 2; b: Interf TC 3, Interf TC 15 and Interf TC 6.

Frequency analysis of calculated data shows that the greatest energy content lies between 0.5Hz and 20Hz, which is a frequency interval where thermal striping may take place, being in good agreement with data detected in the real pipe; anyway frequency spectrum of calculated data does not show any characteristic frequency (see figure 13).

## 7. Conclusions

We have to remark that main results calculated in this work are quite close to those found during IAEA benchmark [3], demonstrating: (i): the reduction of computational cost, because we got results that are comparable with those obtained by participants to the IAEA benchmark performed in the 90', but only using a single powerful PC. (ii): the fact that some RANS turbulence models seem to be reliable in evaluating mean temperature values, even if the quality of such results is very sensitive to the chosen RANS model, (whereas each LES turbulence model provides more or less the same results, limiting the data dispersion). (iii): considering LES runs, the most important improvement in the temperature results has been provided by the adoption of a very long horizontal pipe in the upstream region of the mixing Tee, rather than using different grids or LES subgrid models. Nevertheless, the differences with experimental data are still appreciable, so we think that LES turbulence models should be used very carefully, when they are applied to complex industrial applications. Finally, further developments can be suggested to improve results quality: *first*: it is mandatory to enhance mesh quality (especially in azimuthal and axial direction, in order to decrease elements aspect ratio) and *second*: it could be useful to develop a specific subgrid model for the given problem.

## References

- [1] Naik-Nimbalkar V S, Patwardhan A, W Banerjee I, Padmakumar G and Vaidyanathan G 2010 *Chemical Engineering Science* **65** 5901
- [2] Chellapandi P, Chetal S C, and Baldev R 2009 *Nuclear Engineering and Design* **239** 2754
- [3] IAEA-TECDOC-1318 2002 *Final report of a co-ordinated research project*
- [4] Kuczaj A K, Komen E M, J and Loginov M S 2010 *Nuclear Engineering and Design* **240** 2116
- [5] Munson B R, Young D F, Okiishi T H and Huebsch W W 2012 *Fundamentals of Fluid Mechanics* 6<sup>th</sup> ed John Wiley & Sons Inc;
- [6] Menter F R 2002 *Report EVOL-ECORA-D01*
- [7] Kuhn S, Braillard O, Niceno B, and Prasser H-M 2010 *Nuclear Engineering and Design* **240** 1548
- [8] Ferrara P and Di Marco P 2011 *Proc. XXIX Congresso Nazionale UIT sulla Trasmissione del Calore* Torino
- [9] Ferrara P and Di Marco P 2012 *Proc. Turbulence Heat and Mass Transfer* 7 Palermo
- [10] ANSYS CFX-121 2009 *User Manual* ANSYS Inc.
- [11] Hu L-W and Kazimi M S 2006 *International Journal of Heat and Fluid Flow* **27** 54
- [12] Jackson J D 1983 *International Journal of Heat and Fluid Flow* **4** 107
- [13] Walker C, Simiano M, Zboray R, and Prasser H-M 2009 *Nuclear Engineering and Design* **239** (1) 116
- [14] Hosseini S M, Yuki K and Hashizume H 2008 *International Journal of Heat and Mass Transfer* **51** 2444